Published in: Engineering Structures 85 (2015), pp. 107-117 DOI information: 10.1016/j.engstruct.2014.12.017

Overall Buckling of Lightweight Stiffened Panels Using an Adapted Orthotropic Plate Method

S Benson[1], J Downes[2*], R.S Dow[1]

[1] School of Marine Science and Technology, Newcastle University, UK

[2] Fluid Structure Interactions, Engineering and the Environment, University of Southampton, UK

Abstract

The ultimate longitudinal bending strength of thin plated steel structures such as box girder bridges and ship hulls can be determined using an incremental-iterative procedure known as the Smith progressive collapse method. The Smith method first calculates the response of stiffened panel sub-structures in the girder and then integrates over the cross section of interest to calculate a moment–curvature response curve. A suitable technique to determine the strength behaviour of stiffened panels within the Smith method is therefore of critical importance. A fundamental assumption of the established progressive collapse method is that the buckling and collapse behaviour of the compressed panels within the girder occurs between adjacent transverse frames. However, interframe buckling may not always be the dominant collapse mode, especially for lightweight stiffened panels such as are found in naval ships and aluminium high speed craft. In these cases overall failure modes, where the buckling mode extends over several frame spaces, may dominate the buckling and collapse response. To account for this possibility, an adaptation to large deflection orthotropic plate theory is presented. The adapted orthotropic method is able to calculate panel stress-strain response curves accounting for both interframe and overall collapse. The method is validated with equivalent nonlinear finite element analyses for a range of regular stiffened panel geometries. It is shown how the adapted orthotropic method is implemented into an extended progressive collapse method, which enhances the capability for determining the ultimate strength of a lightweight stiffened box girder.

Keywords: Orthotropic Plate; Progressive Collapse; Buckling; Stiffened Panel; Ultimate Strength; Plates; Nonlinear Finite Element Analysis;

1. Introduction

A critical strength criterion for thin plated girders, such as ship hulls, is their ability to withstand combinations of global bending moment. Box girder structures generally perform equivalently to a long beam, with support conditions depending on the function of the girder. For example a ship is supported continuously by the buoyant volume of the hull, which changes under wave action and causes varying magnitudes of bending moment which is resisted by the longitudinally continuous structure within the hull girder. The maximum wave induced bending moment will usually occur within the mid-section of the hull girder.

The structural design of a box girder must account in some way for the maximum induced bending moment by external load. Girders are now commonly designed using a limit state procedure, which

[*] Corresponding Author. Address: Fluid Structure Interactions, Engineering and the Environment, Southampton Boldrewood Innovation Campus, University of Southampton, Southampton, SO16 7QF, UK. Tel: +44 (0)23 8059 4654. Fax: +44 (0)23 8059 7744. *E-mail address*: jon.downes@soton.ac.uk (J. Downes)

requires an explicit determination of the bending capacity of the longitudinally effective structure. This is often termed the ultimate strength.

A commonly applied technique to calculate the ultimate strength of a thin plated girder is the incremental-iterative approach, which is based on the principles of the simplified progressive collapse method [1,2]. This methodology is an established approach to predict the ultimate capacity of a ship. The method was developed into a rigorous approach for the analysis of ship structures by Smith [2] and the methodology has since been regularly associated with his name. The Smith method first calculates the response of sub-structures within the girder and then integrates over the cross section of interest to calculate a moment–curvature response curve. Progressive collapse is therefore normally governed by the buckling behaviour of the compressed portion of the structure.

The approach used to determine the buckling behaviour of the section is limited by the assumptions inherent in the calculation method such as the longitudinal extents of the section considered and the influence of surrounding structure. Furthermore, because buckling is a nonlinear phenomenon and can be affected by several geometric and material parameters there is a degree of uncertainty inherent in the calculation method.

A key assumption of the Smith method is that the critical failure mode of a hull girder is interframe buckling of the compressed portion of the hull girder. The method, when applied to longitudinally framed ships, is therefore restricted to the analysis of an interframe portion of the hull girder. This has been seen as an acceptable limitation because it is generally assumed that a longitudinally framed hull girder will fail in an interframe manner, with the compressed portion of the girder buckling between adjacent transverse frames. This assertion relies on the transverse frames to be designed sufficiently sturdy to prevent overall buckling modes developing over several frame spaces.

However recent studies have shown, through analytical formulations and nonlinear finite element analysis, that overall buckling may be a possible failure mode in certain ship panels [3]. Overall buckling modes can develop for panels which are either lightly framed or have a large span between strong supports. The development of lightweight ship designs for specialist applications may have particular risk in this regard. A typical example is a car deck on a high speed aluminium ferry (see Figure 1). The deck spans the entire breadth of the ship and is relatively lightly framed. Stanchions support the deck at infrequent intervals and therefore the panel can potentially fail with an overall buckling mode across several frame spaces.

An extension to the progressive collapse method is therefore proposed in Benson et al. [3] which can be used to predict the ultimate strength of a ship's hull girder accounting for buckling over several frame spaces. Fundamental to this procedure is the prediction of the behaviour of the elements within the structure. This paper describes the theoretical basis for the prediction of overall buckling behaviour of compressed panels using an adaptation to large deflection orthotropic plate theory.

Published in: Engineering Structures 85 (2015), pp. 107-117 DOI information: 10.1016/j.engstruct.2014.12.017

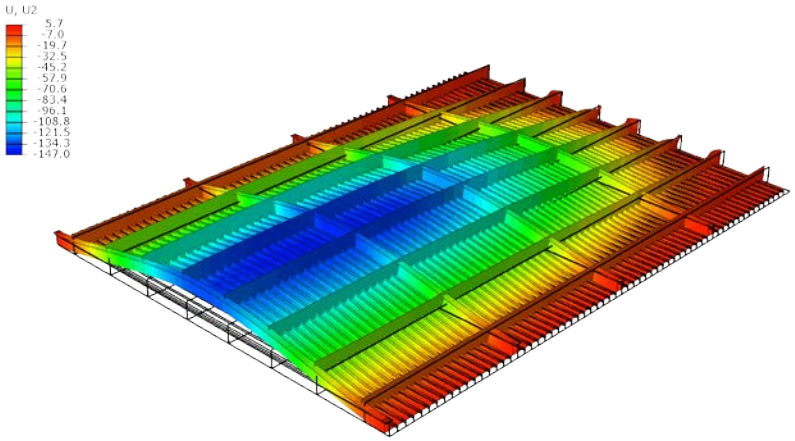

Figure 1 – Example finite element analysis of a deck structure displaying an overall panel buckling mode (displacement magnification x5)

2. Background

The simplified progressive collapse method presented by Dow [4] has been extended by Benson et al. [3] to account for both interframe and overall collapse modes. A key innovation in the extended method concerns the way a girder is subdivided into stiffened panel elements, and then the way the stiffened panel elements are treated within the progressive collapse calculations.

In the progressive collapse method the in plane stress-strain behaviour of each subdivided element is calculated and then used in a summative formula to determine the moment-curvature response of the entire girder. The original progressive collapse method usually subdivides a girder into individual stiffeners with attached plating. The stress-strain response of each plate-stiffener combination is calculated separately. These are then combined in the progressive collapse calculations, meaning that the stress-strain response of each plate-stiffener combination is assumed independent.

The extended progressive collapse method is somewhat different in that it first subdivides a girder into larger scale panels. A panel typically spans between clear corner points in the section and may include a single stiffener type with the same spacing (a regular panel) or several stiffener types with non-uniform spacing (an irregular panel). A typical panel subdivision for a representative ship hull girder section is shown in Figure 2. When placed in compression due to longitudinal bending, each panel within a multi-frame hull girder such as the one shown in Figure 2 may fail either interframe or overall depending on the scantlings. In either case the extended progressive collapse method treats panel strain behaviour consistently throughout the section, assuming all panels have the same length, so that the curvature is incremented appropriately throughout the analysis.

Published in: Engineering Structures 85 (2015), pp. 107-117 DOI information: 10.1016/j.engstruct.2014.12.017

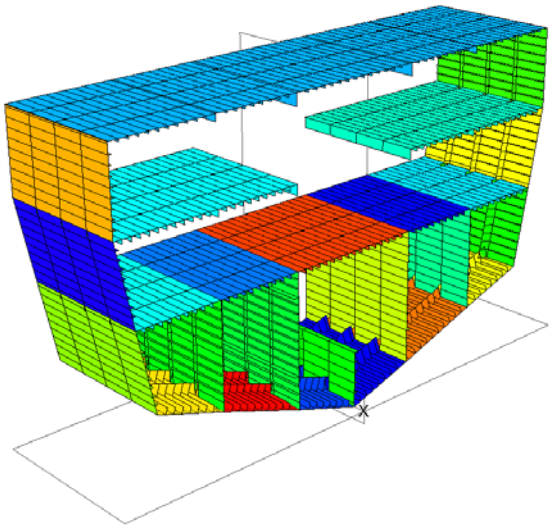

Figure 2 – Example panel sets for a prismatic hull girder

Once the girder is subdivided, a stress-strain curve (also known as a load-shortening curve) is then derived for each panel. The curve describes the nonlinear tensile and compressive behaviour of the panel under uniform uniaxial in-plane load. This is an appropriate description of the panel behaviour when the cross section is placed under pure longitudinal bending, retaining the assumption that the plane section remains plane and that curvature is relatively small. This means that a globally applied bending moment, acting about the instantaneous neutral axis of the girder, produces in plane tension or compression on areas of the cross section above and below the neutral axis accordingly.

The tensile portion of the stress-strain curve is often assumed to replicate the material stress-strain curve of the panel. The influence of residual stresses, imperfections and non-homogenous material properties may affect this assumption, but are not covered in this paper.

The compressive portion of the stress-strain curve defines the buckling and collapse behaviour of the panel. This is almost always nonlinear and, for a relatively slender structure, departs from the material stress-strain curve. The derivation of the compressive stress-strain curve should consider all the relevant failure modes of the panel, including local buckling of the stiffeners or plating, interframe beam column buckling and gross buckling of the panel over several frame spaces. A method to determine the compressive stress-strain curve of a large scale stiffened panel is presented in this paper.

3. Adapted Orthotropic Plate Formulations

A method with the capability to derive the in plane compressive stress-strain curve for an orthogonally stiffened panel must be able to account for all the possible failure modes within the panel. Numerous methods exist for predicting interframe buckling modes such as beam-column failure, stiffener tripping and local plate buckling. Often, in practice, these failure modes interact. For an orthogonal stiffened panel the overall buckling behaviour must also be adequately determined and, if this mode negatively influences the strength of the panel, the stress-strain curve derived accordingly.

Published in: Engineering Structures 85 (2015), pp. 107-117 DOI information: 10.1016/j.engstruct.2014.12.017

An adaptation to the large deflection orthotropic plate method is therefore proposed to predict overall buckling of a stiffened panel. The method is combined with interframe approaches to give a complete algorithm for the derivation of a stress-strain curve for an orthogonal stiffened panel.

3.1. Orthotropic Plate Methods

The orthotropic plate approach is founded on the large deflection plate theory of von Karman and Maguerre [5]. Orthotropic methods treat the plating and stiffeners as an equivalent plate with different elastic properties in the two orthogonal directions. The elastic constants in each direction are calculated assuming the stiffeners are "smeared" into the plating. Solutions to the orthotropic plate problem are presented by Mansour [6], Hughes [7] and Paik et al. [8]. The Classification society DNV-GL has also developed a stiffened panel buckling program, PULS, which uses an orthotropic type modelling approach [9]. The approach presented in this paper differs substantially in the way it treats the elastic constants within the orthotropic calculations.

The orthotropic plate theory has usually been considered more suitable for a panel with a large number of relatively small, closely spaced stiffeners running in both directions. For example, Smith [10] proposed that orthotropic plate theory is valid for simply supported panels with multiple stiffeners in both directions, but less accurate for panels with different edge boundary conditions or with less than three stiffeners in each direction. However, a study by Paik et al. [8] found that a large deflection orthotropic plate method shows good correlation to finite element results for buckling problems between adjacent frames as well as for overall panel buckling of multiple framed panels.

3.2. Large Deflection Orthotropic Plate Equations

The approach presented here is adapted from the derivation originally published by Paik et al. [8]. Key expressions are given in this paper for brevity whilst a full derivation can be found in [8]. The governing nonlinear equations of large deflection orthotropic plate theory are extended from von Karman's original equilibrium and compatibility equations. The form of the governing equations depends on the orthotropic plate method, which range from small deflection linear theory to large deflection nonlinear theory. The large deflection equilibrium and compatibility equations were originally derived by Rostovstev [11] and can be written as:

$$D_x \frac{\partial^4 w}{\partial x^4} + 2H \frac{\partial^4 w}{\partial x^2 \partial y^2} + D_y \frac{\partial^4 w}{\partial y^4} - t\left[\frac{\partial^2 F}{\partial y^2}\frac{\partial^2 (w+w_0)}{\partial x^2} - 2\frac{\partial^2 F}{\partial x \partial y}\frac{\partial^2 (w+w_o)}{\partial x \partial y} + \frac{\partial^2 F}{\partial x^2}\frac{\partial^2 (w+w_0)}{\partial y^2} + \frac{p}{t}\right] = 0 \qquad 1$$

$$\frac{1}{E_y}\frac{\partial^4 F}{\partial x^4} + \left(\frac{1}{G_{xy}} - 2\frac{v_x}{E_x}\right)\frac{\partial^4 F}{\partial x^2 \partial y^2} + \frac{1}{E_x}\frac{\partial^4 F}{\partial y^4} - \left[\begin{array}{c}\left(\frac{\partial^2 w}{\partial x \partial y}\right)^2 - \frac{\partial^2 w}{\partial x^2}\frac{\partial^2 w}{\partial y^2} + 2\frac{\partial^2 w_0}{\partial x \partial y}\frac{\partial^2 w}{\partial x \partial y} \\ -\frac{\partial^2 w_0}{\partial x^2}\frac{\partial^2 w}{\partial y^2} - \frac{\partial^2 w_0}{\partial y^2}\frac{\partial^2 w}{\partial x^2}\end{array}\right] = 0 \qquad 2$$

where D_x and D_y are the flexural rigidities of the plate, H is the torsional rigidity of the plate, F is the Airy stress function, w_0 is the initial deflection of the plate, w is the added deflection of the plate, p is the lateral pressure load, t is the effective plate thickness, E_x and E_y are the elastic moduli of the plate and G_{xy} is the elastic shear modulus of the plate. The subscripts x and y denote longitudinal and transverse directions respectively.

Published in: Engineering Structures 85 (2015), pp. 107-117 DOI information: 10.1016/j.engstruct.2014.12.017

The nonlinear governing equations are a function of the out of plane deflection of the panel, which comprise initial as fabricated deflection (w_o) and added deflection (w) due to buckling. The distribution of deflection across the plate can be expressed by a Fourier series:

$$w_0 = \sum\sum B_{oij}\, sin\frac{i\pi x}{L} sin\frac{j\pi y}{B} \quad 3$$

where B_{oij} is the initial imperfection amplitude for each mode, L is the panel length and B is the panel width.

If a half wave deflection term associated with the panel buckling shape in each direction is assumed dominant, the initial deflection formula can be simplified to include only one buckling mode in x and y. The general case under biaxial in-plane load is:

$$w_0 = A_0\, sin\frac{m\pi x}{L} sin\frac{n\pi y}{B} \quad 4$$

where m and n are the half wave modes in the longitudinal and transverse direction respectively. The buckling mode shape, and hence the value of m and n, depends on the structural orthotropy. If the panel is only loaded in one direction, the half wave mode in the unloaded direction is assumed to be 1. The initial imperfection amplitude, A_0, can be defined using typical statistical representations of panel deflection.

The added deflection can also be defined by a Fourier series with buckling modes as for the initial imperfection. For an arbitrarily loaded panel the added deflection is:

$$w = A_m\, sin\frac{m\pi x}{L} sin\frac{n\pi y}{B} \quad 5$$

where A_m is the added deflection amplitude. To solve the governing equations analytically, the maximum amplitude of the added deflection function must first be obtained.

Both the initial and added deflection shape use a Fourier series shape with a single amplitude value (A_0 and A_m). The use of a single value for A_0 is appropriate when considering a regular stiffened panel with a single plate thickness and stiffener profile as the statistically derived imperfections in the panel are consistent across the entire panel. However, when the method is applied to an irregular stiffened panel (discussed in Section 5) an appropriate assumption needs to be made to represent the average geometric imperfection across the panel. A conservative assumption is to use the highest amplitude imperfection for the panel in question. In any case the initial deflection amplitude makes a relatively minor effect on the eventual result.

Substituting Eq. 4 and Eq. 5 into the compatibility equation (Eq. 2) results in:

$$\frac{1}{E_y}\frac{\partial^4 F}{\partial x^4} + \left(\frac{1}{G_{xy}} - 2\frac{v_x}{E_x}\right)\frac{\partial^4 F}{\partial x^2 \partial y^2} + \frac{1}{E_x}\frac{\partial^4 F}{\partial y^4} = \frac{m^2\pi^4}{2L^2B^2} A_m(A_m + 2A_0)\left(\cos\frac{2m\pi x}{L} + \cos\frac{2n\pi y}{B}\right) \quad 6$$

where F is the Airy stress function, which describes the non-uniform distribution of stress across the plate. The particular solution of the stress function under combined load, obtained by solving Eq. 6, is:

Published in: Engineering Structures 85 (2015), pp. 107-117 DOI information: 10.1016/j.engstruct.2014.12.017

$$F_P = \frac{A_m(A_m + 2A_0)}{32}\left(E_y \frac{n^2L^2}{m^2B^2}\cos\frac{2m\pi x}{L} + E_x \frac{m^2B^2}{n^2L^2}\cos\frac{2n\pi y}{B}\right) \quad 7$$

If uniaxial load in the longitudinal direction is considered, the homogeneous solution which satisfies the loading condition is:

$$F_H = \sigma_{xav}\frac{y^2}{2} \quad 8$$

where σ_{xav} is the average longitudinal stress component in the panel.

The total stress function *F* is the sum of the particular and homogeneous solutions.

$$F = F_P + F_H = \frac{A_m(A_m + 2A_0)}{32}\left(E_y \frac{n^2L^2}{m^2B^2}\cos\frac{2m\pi x}{L} + E_x \frac{m^2B^2}{n^2L^2}\cos\frac{2n\pi y}{B}\right) + \sigma_{xav}\frac{y^2}{2} \quad 9$$

By substituting the stress function (Eq. 9) and deflection equations (Eq. 4 and Eq. 5) into the equilibrium equation (Eq. 1) and applying the Galerkin method then integrating over the entire plate, the continuous problem is converted into a discrete third order equation with respect to the unknown amplitude of the added deflection, A_m.

$$C_1{A_m}^2 + C_2{A_m}^2 + C_3A_m + C_4 \quad 10$$

The solution to this equation is shown in the next section of this paper.

The use of large deflection equations means that the stress distribution over the panel is non-uniform. The panel is assumed to act equivalent to a simply supported plate and therefore it is also assumed the stress distribution follows the same pattern as for the simple plate. The central region of the plate sheds load into the edge regions as the load, and corresponding out of plane deflection, increases. The maximum applied stress at collapse can be assumed to occur at the plate corners whilst the minimum stress is at the centre of the plate edges.

The Airy stress function must satisfy the following conditions at the panel boundaries for σ_x, σ_y, and τ:

$$\sigma_x = \frac{\partial^2 F}{\partial y^2} \quad 11a$$

$$\sigma_y = \frac{\partial^2 F}{\partial x^2} \quad 11b$$

$$\tau = \frac{\partial^2 F}{\partial x \partial y} \quad 11c$$

Thus the stress anywhere along the plate boundary is found by twice differentiating Eq. 9 appropriately. The maximum and minimum stress in the plate can then be calculated directly. Ultimate strength is assumed to be reached when the stress in the plate edges reaches yield. The onset of yielding can be assessed using the von Mises stress criterion, which is defined later in this paper.

3.3. Calculation of Panel Ultimate Strength

Published in: Engineering Structures 85 (2015), pp. 107-117 DOI information: 10.1016/j.engstruct.2014.12.017

The solution to the orthotropic plate equations can be used to evaluate the stress at particular positions on a panel. This section will show that the form of the solution defines the maximum stress at the edge of the panel (σ_{xmax}) as a deviation from the average stress distribution (σ_{xav}) in the panel. For uniaxial compression, the average stress distribution can be directly equated to the externally applied end loading on the panel. Therefore, the equations can be applied iteratively with varying σ_{xav} to converge on the critical load at which the ultimate strength has been reached (indicated by the von Mises stress criterion applied at the plate edges).

The Galerkin method is used to derive the solution to the constants (C_1, C_2, C_3, and C_4) in the discrete equation for longitudinal compression (Eq. 10). A complete solution of this equation using the Cardano method is given by Paik et al. [12]. The resulting constants are a function of the panel geometry (*L, B*), stiffness properties (E_x, E_y, D_x, D_y, G_{xy}, H), deflection shape (A_0, m, n), average stress components ($\sigma_{xav}, \sigma_{yav}$) and lateral pressure (p) is applicable:

$$C_1 = \frac{\pi^2}{16}\left(E_x\frac{m^4B}{L^3} + E_y\frac{n^4L}{B^3}\right) \quad (12)$$

$$C_2 = \frac{3\pi^2 A_0}{16}\left(E_x\frac{m^4B}{L^3} + E_y\frac{n^4L}{B^3}\right) \quad (13)$$

$$C_3 = \frac{\pi^2 {A_0}^2}{8}\left(E_x\frac{m^4B}{L^3} + E_y\frac{n^4L}{B^3}\right) + \frac{m^2B}{L}\sigma_{xav} + \frac{n^2L}{B}\sigma_{yav} + \frac{\pi^2}{t}\left(D_x\frac{m^4B}{L^3} + D_y\frac{n^4L}{B^3} + 2H\frac{m^2n^2}{LB}\right) \quad (14)$$

$$C_4 = A_0\frac{m^2B}{L}\sigma_{xav} + A_0\frac{n^2L}{B}\sigma_{yav} - \frac{16LB}{\pi^4 t}p \quad (15)$$

The discrete solution of the third order equation can be found using standard algebraic methods and results in:

$$A_m = \frac{C_2}{3C_1} + k_1 + k_2 \quad (16)$$

where:

$$k_1 = \left(-\frac{Y}{2} + \sqrt{\frac{Y^2}{4} + \frac{X^3}{27}}\right)^{1/3} \quad (17)$$

$$k_2 = \left(-\frac{Y}{2} - \sqrt{\frac{Y^2}{4} + \frac{X^3}{27}}\right)^{1/3} \quad (18)$$

$$X = \frac{C_3}{C_1} - \frac{{C_2}^2}{3{C_1}^2} \quad (19)$$

$$Y = \frac{2{C_2}^2}{27{C_1}^2} - \frac{C_2C_3}{3{C_1}^2} + \frac{C_4}{C_1} \quad (20)$$

To establish a discrete solution from the equations above the critical buckling mode shape must be calculated. As shown in Eq. 4 and Eq. 5, this is defined by the buckling mode numbers *m* and *n*. The transverse shape (defined by *n*) can be assumed to be unity, giving a half sine wave shape across the

width. However, the longitudinal shape (defined by *m*) is a function of the buckling mode. To find the critical value of m a special case of Eq. 10 is solved setting the initial deflection A_0 to zero. Without the initial deflection the total panel deflection just prior to collapse will also be zero. The resulting solution of Eq. 10 is:

$$A_m = \sqrt{-\frac{C_3}{C_1}} = 0 \tag{21}$$

where the constants C_1 and C_3 are in a reduced form because n=1 and A_0=0:

$$C_1 = \frac{\pi^2}{16}\left(E_x \frac{m^4 B}{L^3} + E_y \frac{L}{B^3}\right) \tag{22}$$

$$C_3 = \frac{m^2 B}{L}\sigma_{xav} + \frac{\pi^2}{t}\left(D_x \frac{m^4 B}{L^3} + D_y \frac{L}{B^3} + 2H\frac{m^2}{LB}\right) \tag{23}$$

The solution of Eq. 22 is when $C_3 = 0$. Rearranging, this gives:

$$\sigma_{xav} = D_x \frac{m^2}{L^2} + 2H\frac{1}{B^2} + D_y \frac{L^2}{m^2 B^4} \tag{24}$$

The critical value of m can then be found to give the minimum value of σ_{xav}, satisfying the following equations:

$$D_x \frac{m^2}{L^2} + 2H\frac{1}{B^2} + D_y \frac{L^2}{m^2 B^4} \leq D_x \frac{(m+1)^2}{L^2} + 2H\frac{1}{B^2} + D_y \frac{L^2}{(m+1)^2 B^4} \tag{25}$$

Once m is known the discrete solution of the third order equation for the added deflection, A_m, can be calculated.

The stress distribution over the whole orthotropic panel is then computed by substituting A_m into the Airy stress function (Eq. 9) and using Eq. 11 to produce:

$$\sigma_{x\,max} = \sigma_{xav} - \frac{m^2\pi^2 E_x A_m (A_m + 2A_0)}{8L^2} \tag{26}$$

$$\sigma_{x\,min} = \sigma_{xav} + \frac{m^2\pi^2 E_x A_m (A_m + 2A_0)}{8L^2} \tag{27}$$

$$\sigma_{y\,max} = \sigma_{yav} - \frac{n^2\pi^2 E_y A_m (A_m + 2A_0)}{8B^2} \tag{28}$$

$$\sigma_{y\,min} = \sigma_{yav} + \frac{n^2\pi^2 E_y A_m (A_m + 2A_0)}{8L^2} \tag{29}$$

The non-dimensional von Mises stress criterion can be used to assess the stress state at any point in the plate. The maximum stress in a uniaxial compressed orthotropic plate is at the midpoint of the longitudinal edges. At this point the von Mises stress, σ_{MISES}, is:

$$\left(\frac{\sigma_{xmax}}{\sigma_0}\right)^2 - \left(\frac{\sigma_{xmax}}{\sigma_0}\right)\left(\frac{\sigma_{ymin}}{\sigma_0}\right) + \left(\frac{\sigma_{ymin}}{\sigma_0}\right)^2 = \frac{\sigma_{MISES}}{\sigma_0} \tag{30}$$

Published in: Engineering Structures 85 (2015), pp. 107-117 DOI information: 10.1016/j.engstruct.2014.12.017

Collapse is indicated when the von Mises stress equals the material yield or proof stress (i.e. σ_{MISES}/σ_0=1). If the von Mises stress is less than yield then the assumed average edge stress is too low. A von Mises stress greater than yield indicates the opposite. The calculations are therefore iterated with revised predictions of σ_{ave} based on the predictions of Eq. 30.

Once the iterations have reached an acceptable convergence, the instantaneous strength of the panel for the overall failure mode can be simply calculated. For uniaxial compression this is

$$R_O = \sigma_{xav} A \quad (31)$$

where *A* is the cross section area of the panel.

A flow chart showing the calculation process is given in Figure 3. The orthotropic calculations require the panel stiffness and flexure parameters as an input.

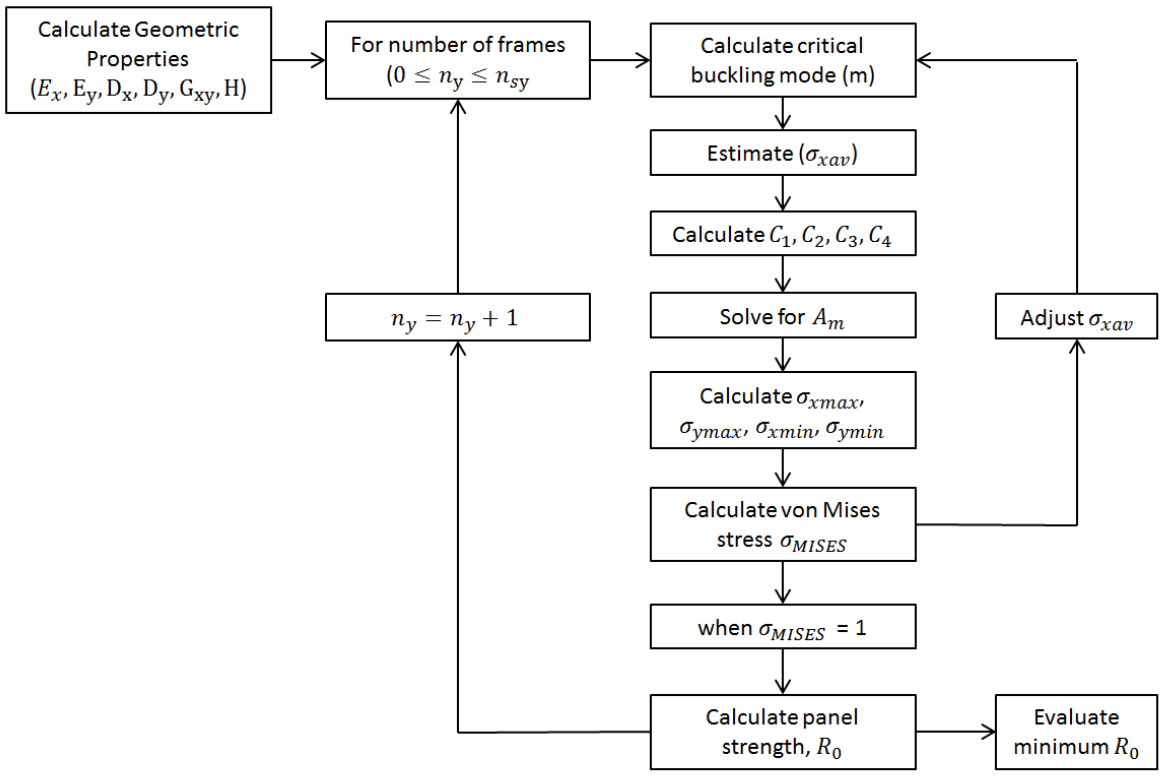

Figure 3 – Orthotropic Plate Calculation Flow Chart

3.4. Orthotropic Panel Properties

As shown in Fig. 3, the overall panel strength, R_O, is a function of the orthotropic geometric properties, which are themselves functions of the various elastic constants of the orthotropic plate. The elastic constants in an isotropic plate comprise the Young's modulus, *E*, and the Poisson ratio, *v*. For an orthotropic plate, separate constants in the *x* and *y* directions must be defined, to take into account the anisotropy arising from the different geometry. These are the stiffness (E_x and E_y),

Poisson ratio (v_x and v_y), flexural rigidity (D_x and D_y), torsional rigidity (H) and elastic shear modulus (G_{xy}).

These constants reflect the orthotropy of the resulting plate when including the equivalent "smeared" effect of the individual stiffeners. The equations are derived using the governing nonlinear differential equations of large deflection orthotropic flat plate theory. In the classical method, these quantities are functions of the panel geometry and the material Young's modulus. The method assumes that the material properties remain elastic when placed under load. The method thus predicts the elastic response of the panel only.

This assumption is reasonable for very light stiffened panels, where buckling and collapse occur elastically with average edge stress well below the material yield point. However, this assumption is less acceptable when applied to more stocky stiffened panels. In these cases, the response of the panel involves elasto-plastic collapse mechanisms. This means that, even before buckling, the stiffness and rigidity of the plating and stiffeners changes, usually adversely, as the panel is compressed. The nonlinear behaviour of the component stiffness must be properly accounted for as a reduction in component stiffness has a corresponding reduction in the overall panel strength R_O.

Therefore, in the adapted method, the effective equivalent stiffness and flexural properties of the panel components are given as a function of the end displacement of the panel. These are re-derived as instantaneous stiffness and flexural rigidity values using the tangent stiffness' of the panel components. The overall panel strength becomes a function of the tangent stiffness of the plating and the stiffeners:

$$R_O(u) = f\left(E_{T_p}, E_{T_s}\right) \tag{32}$$

The tangent stiffness' of the components are themselves a function of the end displacement of the panel and are calculated using datasets as explained in the next section of this paper.

As the panel end displacement increases, the local tangent modulus of the component stress-strain curve reduces, causing a corresponding reduction in the orthotropic plate stiffness values. Similarly, and often more importantly in determining the strength, the flexural rigidity of the components are also affected.

The instantaneous stiffnesses in *x* and *y* for the panel under longitudinal compressive load are therefore defined as:

$$E_x = \frac{E_{T_p} B t_p + E_{T_s} n_{sx} A_{sx}}{B t_p} \tag{33}$$

$$E_y = \frac{E_{T_p} L t_p + E_{T_s} n_{sy} A_{sy}}{L t_p} \tag{34}$$

E_{Tp} is the instantaneous tangent modulus from the plate component stress-strain curve. Likewise, E_{Ts} is the tangent modulus from the stiffener stress-strain curve. It is assumed the longitudinal plate tangent stiffness adequately represents the plate in the calculation of E_x and E_y, although strictly speaking E_{Tp} only describes the longitudinal stiffness of the panel. This was considered a reasonable

assumption because biaxial plate tests show a reduction in plate stiffness in the transverse direction if a load has previously been applied in the longitudinal direction.

However, this assumption cannot be applied to the transverse frames. The transverse stiffeners are represented by $E_{(\sigma-\varepsilon)}$, which is the tangent modulus of the material stress-strain curve. This is usually equivalent to the elastic Young's modulus for steel and the tangent modulus of the Ramberg Osgood [13] stress-strain curve for aluminium. This assumes that the transverse frame does not experience high levels of strain, which is reasonable when the load is in the longitudinal direction only.

The orthotropic Poisson's ratio equations are similarly defined as:

$$M = \frac{E_y}{E_x}\left(\frac{E_{T_p}t^3}{12} + E_{T_p}t{z_{0x}}^2 + \frac{E_{T_s}I_x}{b}\right) - \frac{E_{T_p}t^3}{12} - E_{T_p}t{z_{0y}}^2 - \frac{EI_y}{a} \quad (35)$$

$$N = \frac{E_{T_s}I_x}{b}\left(\frac{E_y}{E_x}\right)^2 - \frac{EI_y}{a}\left(\frac{E_y}{E_x}\right) \quad (36)$$

$$v_x = c\left[\frac{M}{N}\right]^{0.5} \quad (37)$$

$$v_y = \frac{E_y}{E_x}v_x \quad (38)$$

$$v_{xy} = \sqrt{v_x v_y} \quad (39)$$

The second moment of area is calculated as:

$$I_x = b_p{t_p}^3 + b_p t_p\left(z_0 - \frac{t_p}{2}\right)^2 + t_w{h_w}^3 + t_w h_w\left(z_0 - t_p - \frac{h_w}{2}\right)^2 + b_f{t_f}^3 + b_f t_f\left(z_0 - t_p - h_w\frac{t_f}{2}\right)^2 \quad (40)$$

The calculation of the orthotropic Poisson ratio can break down as the component stiffness progressively reduces. If the result of either Eq. 37 or 38 becomes negative then the solution of Eq. 37 is no longer real. This usually occurs when the panel has surpassed the peak collapse load, and thus only impacts on the post collapse part of the stress-strain curve. Therefore, to handle the problem, the incremental procedure checks for negative values of *M* and *N* at each successive increment, and if either becomes negative, then the previous increment value is used in Eq. 37 to keep υ_{xy} real.

The tangent and torsional rigidities and the shear modulus of the orthotropic plate are also reworked as follows:

$$D_x = \frac{E_{T_p}t^3}{12\left(1 - v_{xy}^2\right)} + \frac{E_{T_p}t{z_0}^2}{1 - v_{xy}^2} + \frac{E_{T_s}I_x}{b} \quad (41)$$

$$D_y = \frac{E_{T_p}t^3}{12\left(1 - v_{xy}^2\right)} + \frac{E_{T_p}t{z_0}^2}{1 - v_{xy}^2} + \frac{EI_y}{a} \quad (42)$$

$$G_{xy} = \frac{\sqrt{E_x E_y}}{2\left(1 + \sqrt{v_x v_y}\right)} \quad (43)$$

Published in: Engineering Structures 85 (2015), pp. 107-117 DOI information: 10.1016/j.engstruct.2014.12.017

$$H = \frac{1}{2}\left(v_y D_x + v_x D_y + G_{xy}\frac{t^3}{3}\right) \quad (44)$$

3.5. Component Stress-Strain Curve Datasets

The adapted orthotropic plate approach requires information on the stiffness behaviour of the plate and stiffener components. These are taken from plate [14] and stiffener [15] datasets. An example dataset for unstiffened plates are shown in Figure 4. Curves are presented for three levels of initial imperfection (slight, average, severe) which are based on statistical measurements [16].

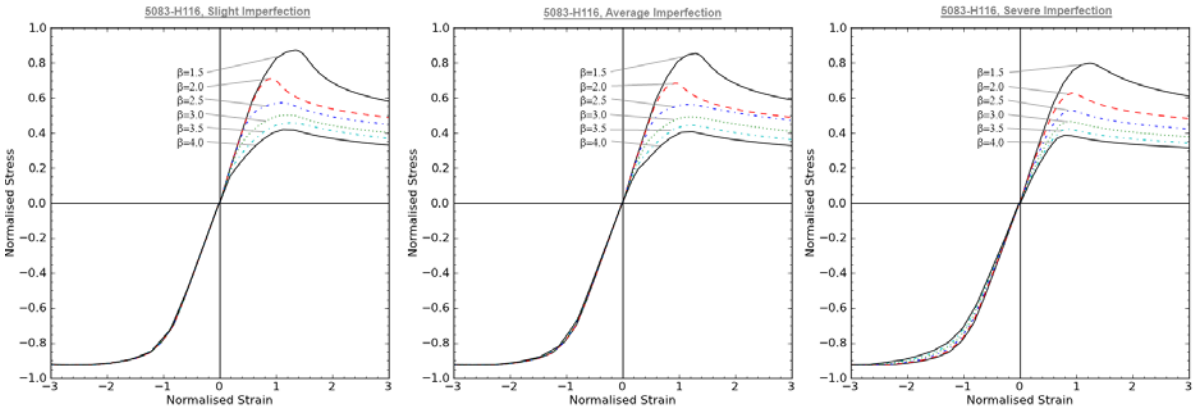

Figure 4 – 5083-H116 plate stress-strain curves with slight (left), average (centre) and severe (right) imperfections. Source: [14]

The individual plate and stiffener stress-strain curves are derived by interpolating within the numerical datasets. Linear interpolation gives adequate accuracy as long as the datasets are sufficiently detailed.

Once defined, the plate and stiffener component curves are used to give a measure of the instantaneous resistance of the component to a given end displacement (R_P and R_S) and to define the instantaneous tangent stiffness of the components (E_{Tp} and E_{Ts}). An example plate curve is presented in Figure 5 with a visual definition of the tangent modulus.

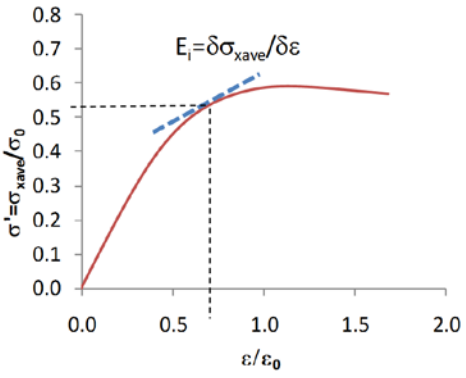

Figure 5 – Example measurement of component resistance and tangent modulus

4. Stress-Strain Curve Derivation

Published in: Engineering Structures 85 (2015), pp. 107-117 DOI information: 10.1016/j.engstruct.2014.12.017

The adapted orthotropic plate method produces an overall panel strength value as a function of the end displacement. This must be recalculated for incremental steps of end displacement and compared to the equivalent resistance of the panel at each step. This enables the entire stress-strain curve for the panel to be developed.

The panel resistance to a given end displacement is calculated as a combination of the resistance from the plating and stiffeners.

The plate resistance, R_P, is a function of the end shortening displacement and is calculated by converting the normalised stress-strain relationship to a stress-strain relationship:

$$R_{plate}(u) = \sigma_s'(u)\sigma_0 b t_p \quad (45)$$

where:

$$u = \varepsilon' \varepsilon_0 a \quad (46)$$

Likewise, the stiffener resistance is also derived using a representative predefined dataset and converted into the load-shortening format as follows:

$$R_{stiff}(u) = \sigma_s'(u)\sigma_0\left(h_w t_w + b_f t_f\right) \quad (47)$$

The contribution of the stiffener and the plate to the combined local panel resistance, R_L, is proportional to the relative sectional area of the two components and can be calculated as:

$$R_L(u) = \frac{R_{plate}(u) bt + R_{stiff}(u)\left(h_w t_w + b_f t_f\right)}{bt + h_w t_w + b_f t_f} \quad (48)$$

At each increment of end displacement, the instantaneous overall panel resistance, *R(u)* is determined as the lesser of R_O and R_L.

In the first (pre collapse) increments of the calculations, R_L should remain the lesser value. The panel stiffness remains positive and the stress-strain curve follows the Plate and Stiffener Combination (PSC) representation. R_{PO} is usually a fairly high value, particularly if the panel is reasonably stocky. This is because the component properties are in the elastic region and the orthotropic calculations are thus reporting the elastic overall buckling strength of the panel.

As end displacement increases, several possibilities may occur. In some instances the overall panel resistance remains higher than the local panel resistance throughout the displacement range. If this is the case, the panel is judged to collapse interframe and the local panel curve is used to represent the behaviour throughout. This is sketched in Figure 6a, which plots the panel curve together with the overall panel strength determined over the entire displacement range.

In other instances, the local panel resistance exceeds the instantaneous overall panel strength prior to interframe collapse. This signals a switch from interframe to an overall mode of failure, and also usually determines the ultimate strength of the panel. This is shown in Figure 6b - Figure 6d. The overall failure mode becomes critical where the panel strength curve intersects with the stress-strain curve. At this point a separate post collapse algorithm is used, which will be explained below. The switch to overall buckling can be due to several different phenomena predicted by the extended orthotropic plate calculations. In some cases, the elastic properties of the orthotropic plate are such

Published in: Engineering Structures 85 (2015), pp. 107-117 DOI information: 10.1016/j.engstruct.2014.12.017

that the overall mode of collapse starts from a low value. Thus the positive gradient of the stress-strain curve meets the overall panel strength curve which remains horizontal (Figure 6b).

In other instances, the overall panel strength curve initially predicts a high ultimate strength. However, the reduction in the stiffness properties of the components causes the strength curve to descend as shown in Figure 6c and Figure 6d. This often occurs quite rapidly, as either the plate or stiffener start to reduce in stiffness and approach their local buckling points. In this case the intersection with the stress-strain curve is due to the negative gradient in the overall panel strength curve. The intersection point may occur prior to the ultimate strength point (Figure 6c) or after the ultimate strength point has been passed (Figure 6d).

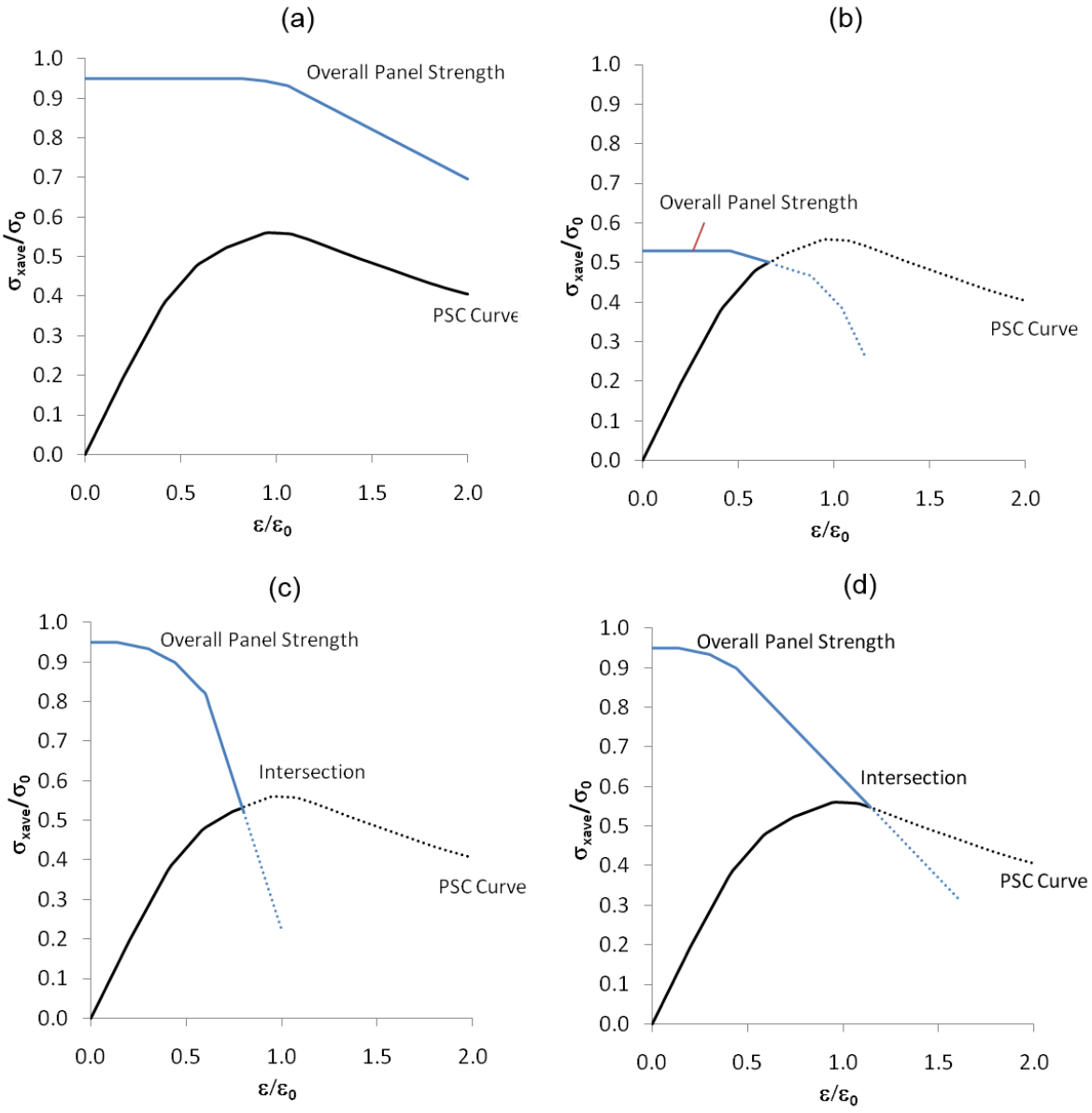

Figure 6 – Example PSC and overall panel strength curves

Published in: Engineering Structures 85 (2015), pp. 107-117 DOI information: 10.1016/j.engstruct.2014.12.017

The intersection point determines the ultimate strength of the orthogonal panel and indicates an overall collapse mode. The post collapse behaviour of the panel is also required to complete the stress-strain curve prediction over the entire displacement range.

The post collapse curve is calculated by taking the initial gradient from the post collapse point and assuming a linear post collapse curve shape. The gradient of the post collapse response is thus determined by the orthotropic plate behaviour in the ultimate strength region only. Thus a steep post collapse gradient is predicted when overall panel strength drops steeply due to plasticity in the components. When the panel is very lightly framed, and the ultimate strength point is well within the elastic region, the post collapse gradient is much shallower. An example of this type of collapse is shown in Figure 6b.

5. Irregular Stiffened Panels

The adapted orthotropic plate method as described applies to a regularly stiffened panel. For panels with several different stiffeners making up the cross section a further extension of the method is required.

The primary inputs to the adapted method are stress-strain curves which describe the component behaviour. In the method as described so far, these components are simple flat plates and single stiffeners. The stiffener shape is important for determining the second moment of area of the panel and hence the panel slenderness. However, the actual shape of the plate component is not so important. Therefore, an “equivalent” plate can be used, which is actually a span of stiffened structure.

The output of the method is overall panel strength, where the individual plates and stiffeners are treated as a single entity, which is then used to construct a stress-strain curve for the panel. This allows an irregular stiffened panel to be analysed by using multiple passes through the orthotropic plate method. Each pass uses larger model extents to encompass more structure. The previous model extents are represented by the associated stress-strain curve and are treated as equivalent to a simple plate. After each pass the strength of the larger model is compared to the previous intermediate model. A reduced strength behaviour indicates that the stiffeners in the larger model do not provide sufficient lateral support and must be included as part of the panel buckling analysis.

This is shown diagrammatically in Figure 7. A span of regularly stiffened plating between deep longitudinals is first analysed using the semi analytical method. This sub panel is assigned a stress-strain curve from the results of the first pass analysis. The intermediate span is then treated as an equivalent plate attached to the deep longitudinals, with the plate behaviour represented by the intermediate level panel stress-strain curve. A second pass through the orthotropic calculations is completed.

Published in: Engineering Structures 85 (2015), pp. 107-117 DOI information: 10.1016/j.engstruct.2014.12.017

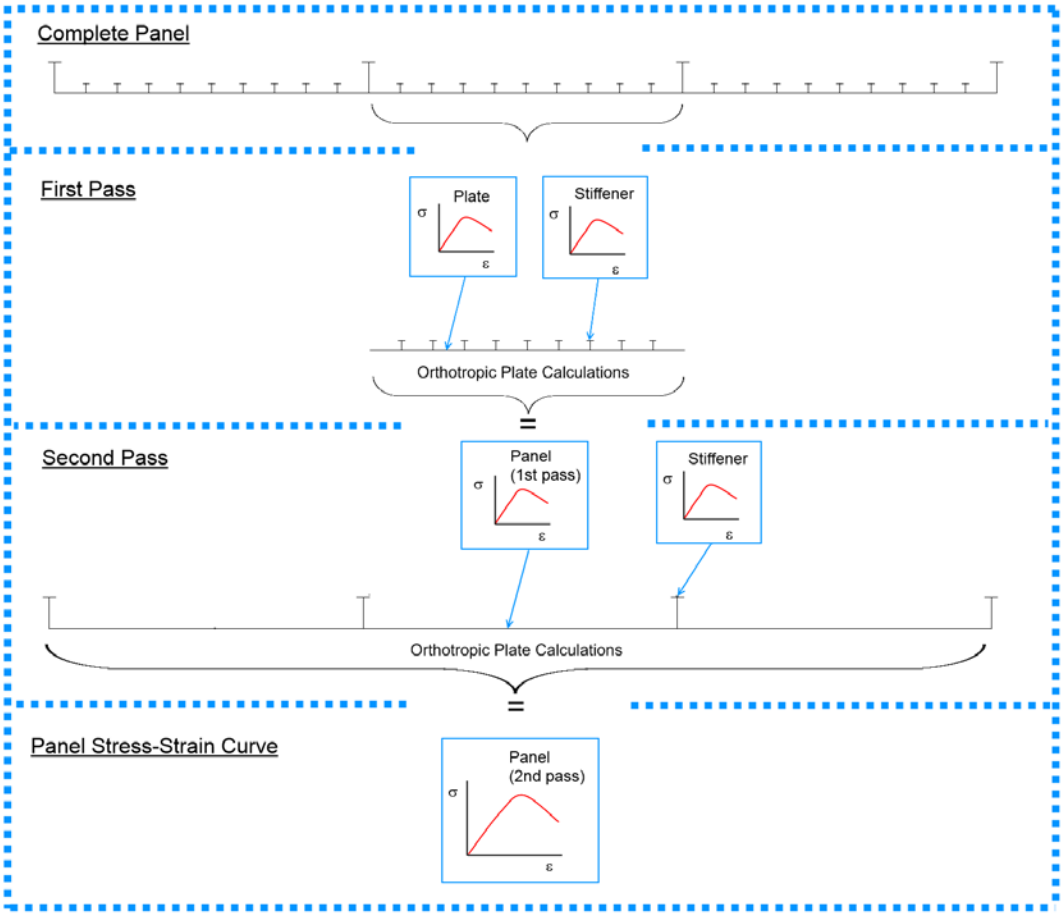

Figure 7 – Irregular panel calculation flow diagram

6. Validation

A series of orthogonally stiffened flat panels, with dimensions as shown in Table 1, were tested in uniaxial compression using the adapted orthotropic plate method and compared to equivalent numerical results using nonlinear finite element analysis. Full details of the finite element analysis methodology and model setup are found in Benson [15] and only a brief summary is given here. The panels were developed with a range of plate and column slenderness. Both steel and aluminium panels were tested. All finite element analyses, completed using ABAQUS 6.12, included explicit consideration of the geometric imperfections, weld induced residual stress and for the aluminium panels the inclusion of a reduced strength heat affected zone adjacent to welded joints. These parameters are consistent with those used to develop the plate and stiffener load shortening curves for the adapted orthotropic method. Boundary conditions were set with simple supports and imperfection seeded into the panel model to ensure collapse nucleated in the central region of the panel away from the boundaries. All finite element models used 4 node reduced integration elements. A static implicit solver using the arc length technique was used to ensure convergence through to the post-buckling region.

The comparative ultimate strengths predicted by the two comparative approaches are presented graphically in Figure 8 and tabulated in Table 2. The results show reasonably good correlation. The

Published in: Engineering Structures 85 (2015), pp. 107-117 DOI information: 10.1016/j.engstruct.2014.12.017

adapted orthotropic plate approach is conservative with a mean bias of 0.93. The coefficient of variation (COV) is 0.14 which is of similar order to other comparative studies.

Table 1 - Case Study Panels

Dataset ID	*Mat.*	*a* (mm)	*b* (mm)	t_p (mm)	h_w (mm)	t_w (mm)	b_f (mm)	t_f (mm)	λ (mm)	β (mm)	A_s/A
M1	5083	1200	400	14.8	120	5.5	55	7.7	0.62	1.5	0.15
M2	5083	1200	400	11.1	120	5.5	55	7.7	0.56	2.0	0.20
M3	5083	1200	400	8.9	120	5.5	55	7.7	0.53	2.5	0.23
M4	5083	1200	400	7.4	120	5.5	55	7.7	0.50	3.0	0.27
M5	5083	1200	400	14.8	80	4.5	45	6.2	1.09	1.5	0.10
M6	5083	1200	400	14.8	170	6.5	65	10.3	0.38	1.5	0.23
M7	5083	1000	400	14.8	120	5.5	55	7.7	0.52	1.5	0.15
M8	5083	1800	400	14.8	120	5.5	55	7.7	0.93	1.5	0.15
M9	5083	1200	800	14.8	120	5.5	55	7.7	0.81	3.0	0.08
M10	5083	1200	500	14.8	120	5.5	55	7.7	0.67	1.87	0.13
S1	Steel	2281	510	11.6	120	5.5	55	7.7	0.62	1.5	0.15
S2	Steel	2281	510	8.7	120	5.5	55	7.7	0.56	2.0	0.20
S3	Steel	2281	510	7.0	120	5.5	55	7.7	0.53	2.5	0.23
S4	Steel	2281	510	5.8	120	5.5	55	7.7	0.50	3.0	0.27

Published in: Engineering Structures 85 (2015), pp. 107-117 DOI information: 10.1016/j.engstruct.2014.12.017

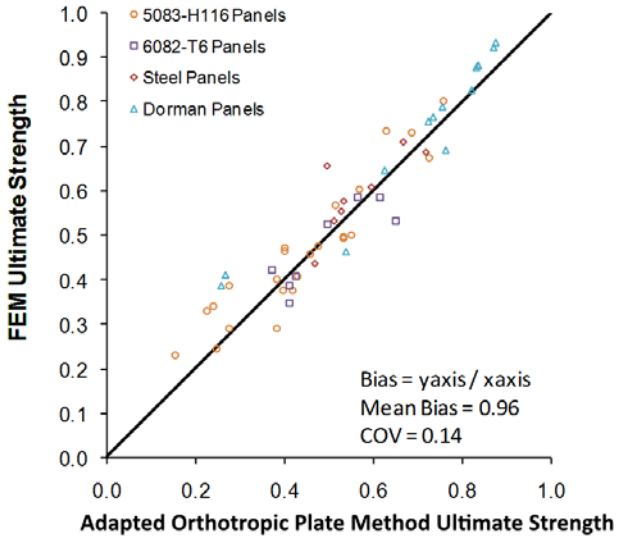

Figure 8 – Comparative panel buckling results

Table 2 - Case Study Results

Panel ID	*Frame Dims (mm)*	*Ult. Strength (FEM)*	*Ult. Strength (Simplified)*
M1	360x10	0.71	0.69
M1	180x10	0.36	0.43
M2	360x10	0.66	0.63
M2	180x10	0.46	0.46
M3	360x10	0.61	0.57
M3	180x10	0.47	0.40
M4	360x10	0.56	0.51
M4	180x10	0.46	0.40
M5	360x10	0.38	0.42
M5	180x10	0.24	0.25
M6	360x10	0.80	0.76
M6	180x10	0.50	0.55
M7	360x10	0.67	0.73
M7	180x10	0.38	0.40

M8	360x10	0.50	0.53
M8	180x10	0.40	0.38
M9	360x10	0.33	0.16
M9	180x10	0.23	0.22
M10	360x10	0.47	0.48
M10	180x10	0.34	0.24
S1	360x10	0.69	0.72
S1	180x10	0.44	0.47
S2	360x10	0.71	0.67
S2	180x10	0.66	0.50
S3	360x10	0.61	0.60
S3	180x10	0.55	0.53
S4	360x10	0.58	0.53
S4	180x10	0.53	0.51

For the purposes of providing input to the extended progressive collapse method, the curve shape produced by the simplified method is also highly important. Example stress-strain curves for panels M2 are shown in Figure 9 and Figure 10. Three curves are shown in each Figure. The plate-stiffener combination (PSC) curve is produced using a simple FEM model with a single stiffener and attached plating. The multi-frame panel FEM curve is a large scale finite element model with 20 longitudinal stiffeners and 8 transverse frames. Finally the result from the adapted orthotropic plate method is also shown. An image of the panel buckling mode from the FEM analyses is also shown, which shows a clear overall buckling mode with the smaller transverse frame and a more interframe type of collapse with the stockier frame. However, it is clear from the stress-strain curves that both panels fail in an overall manner when compared to the equivalent PSC curves. This is confirmed in the adapted orthotropic plate method result, which closely tracks the multi-frame panel FEM curve.

These plots demonstrate that, for the panels tested, the adapted orthotropic plate method generally predicts a good curve shape over the entire load range. In the pre-collapse region of the curve, the semi analytical method tracks closely to the PSC result. The ultimate strength point forms a sharp transition into the post collapse curve. The sharp peak is always more pronounced than the more rounded peak of the FEM results. The linear post-collapse relationship, as predicted by the analytical method, shows reasonably close correlation to the FEM results. For example, the panel stress-strain curve for M2 changes from a relatively sharply peaked post collapse relationship when predominantly failing interframe to a shallow post-collapse response (with a much lower ultimate

strength) when failing in an overall buckling mode. This is well predicted by the adapted orthotropic plate method.

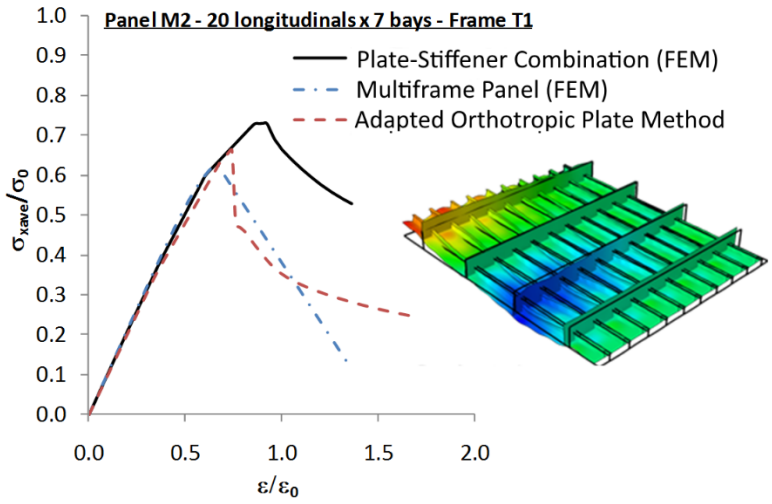

Figure 9 – Panel stress-strain curves: M2 with 360x10 frames

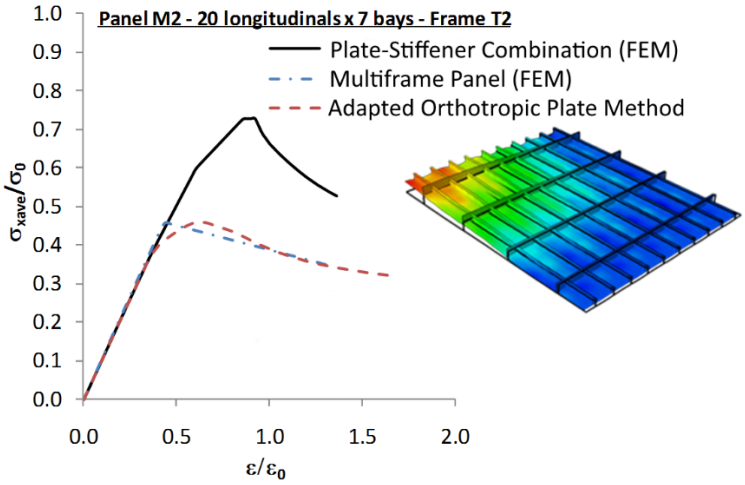

Figure 10 – Panel stress-strain curves: M2 with 180x10 frames

7. Conclusions

The extended progressive collapse method overcomes a fundamental limitation, namely that the buckling behaviour of the compressed portion of a thin plated orthogonally stiffened girder under longitudinal bending moment occurs between adjacent transverse frames. This may not always be an adequate assumption, especially for lightweight ships such as naval vessels and aluminium high speed craft. Overall failure modes, where the buckling mode extends over several frame spaces, can be accounted for in the progressive collapse method by adapting the stress-strain curves which describe the behaviour of the panel elements making up the longitudinal hull girder. The use of large scale panels to define the stress-strain relationship of the structural elements requires an analytical method to predict both overall and interframe buckling modes. An adapted orthotropic plate

method has been developed to meet this demand. The method is capable of defining a complete stress-strain relationship for an orthogonal stiffened panel accounting for the elasto-plastic properties of the plate and stiffener components. The method demonstrates good agreement to equivalent nonlinear finite element analyses of large scale stiffened panels in uniaxial compression. The method has been developed for specific applicability to large lightweight ship hulls but may also find application in other thin plated structures such as box girder bridges and offshore structures.

8. Acknowledgments

The Authors gratefully acknowledge the support of the U.S. Office of Naval Research (ONR) under Funding Grant: N00014-07-1-0533.

9. References

[1] J.B. Caldwell, Ultimate Longitudinal Strength, Trans. R. Inst. Nav. Archit. 107 (1965) 411–430.

[2] C.S. Smith, Influence of local compressive failure on ultimate longitudinal strength of a ship's hull, PRADS 1977. (1977) 73–79.

[3] S. Benson, J. Downes, R.S. Dow, Compartment level progressive collapse analysis of lightweight ship structures, Mar. Struct. 31 (2013) 44–62.

[4] R.S. Dow, Structural Redundancy and damage tolerance in relation to ultimate ship hull strength, Adv. Mar. Struct. 3. (1997).

[5] F. Bleich, Buckling Strength of Metal Structures, McGraw Hill, 1952.

[6] A. Mansour, Gross Panel Strength Under Combined Loading, Ship Structure Committee, 1977.

[7] O.F. Hughes, Ship structural design : a rationally-based, computer-aided optimization approach , Jersey City, N.J. : Society of Naval Architects and Marine Engineers, 1988.

[8] J.K. Paik, A.K. Thayamballi, B. Ju Kim, Large deflection orthotropic plate approach to develop ultimate strength formulations for stiffened panels under combined biaxial compression/tension and lateral pressure, Thin-Walled Struct. 39. 2001. 215–246.

[9] E. Steen, E. Byklum, K.G. Vilming, Computer Efficient Non-Linear Buckling Models for Capacity Assessments of Stiffened Panels Subjected to Combined Loads, 2004.

[10] C. S. Smith, "Elastic Buckling and Beam Column Behaviour of Ship Grillages," Trans. R. Inst. Nav. Archit., vol. 110, pp. 127–147, 1968.

[11] G.. Rostovtsev, Calculation of a Thin Plane Sheeting supported by Ribs, Tr Leningr. Inst. Inzhenerov Gradhdanskogo Vosdushnogo Flot. 1940.

[12] J. K. Paik, A. K. Thayamball, and D. H. Kim, "An analytical method for the ultimate compressive strength and effective plating of stiffened panels," J. Constr. Steel Res., vol. 49, pp. 43–68, 1999.

[13] Ramberg, W., and W.R. Osgood. “Description of Stress-Strain Curves by Three Parameters”, National Advisory Committee For Aeronautics, Washington DC, 1943.

[14] S. Benson, J. Downes, R.S. Dow, Load shortening characteristics of marine grade aluminium alloy plates in longitudinal compression, Thin-Walled Struct. 70 (2013) 19–32.

[15] S. Benson, Progressive Collapse Assessement of Lightweight Ship Structures, Newcastle University, PhD Thesis, 2011.

[16] C.S. Smith, N. Anderson, J.C. Chapman, P.C. Davidson, P.J. Dowling, Strength of stiffened plating under combined compression and lateral pressure, Trans. R. Inst. Nav. Archit. (1991) 131–147.